

Electrospun Fibers of Functional Nanocomposites Composed of Single-Walled Carbon Nanotubes, Fullerene Derivatives, and Poly(3-Hexylthiophene)

Céline Bounioux,¹ Racheli Itzhak,² Ron Avrahami,³ Eyal Zussman,³ Joseph Frey,⁴ Eugene A. Katz,^{1,5} Rachel Yerushalmi-Rozen^{2,5}

¹Department of Solar Energy and Environmental Physics, Jacob Blaustein Institutes for Desert Research, Ben-Gurion University of the Negev, Sede Boker Campus 84990, Israel

²Department of Chemical Engineering, Ben-Gurion University of the Negev, Beer-Sheva 84105, Israel

³Department of Mechanical Engineering, Technion, Haifa 32000, Israel

⁴Department of Chemistry and Institute for Nanotechnology and Advanced Materials, Bar Ilan University, Ramat Gan 52900, Israel

⁵The Ilze Katz Institute for Nanoscale Science and Technology, Ben-Gurion University of the Negev, Beer-Sheva 84105, Israel

Correspondence to: R. Yerushalmi-Rozen (E-mail: rachely@bgu.ac.il)

Received 8 January 2011; revised 1 May 2011; accepted 3 May 2011; published online 27 May 2011

DOI: 10.1002/polb.22281

ABSTRACT: Electrospinning of fibers composed of poly(3-hexylthiophene) (P3HT), fullerene derivative, phenyl-C₆₁-butyric acid methyl ester (PCBM), and single-walled carbon nanotubes (SWNT) is reported. While of great promise for photovoltaic applications, morphological control of functional structures is a great challenge for most processing methods. It is demonstrated that the use of a tailor-made block-copolymer for dispersion of individual SWNT enables the preparation of stable dispersions of individual tubes that may be further cospun from chloroform solutions with PCBM and P3HT into submicron fibers. The block copolymer

used to mediate the colloidal and interfacial interactions in the combined system enables the spinning of centimeters long and uniform fibers. Structural characterization indicates a high degree of ordering and alignment within the fibers and absorption and quenching of the photoluminescence indicate significant interactions among the components. © 2011 Wiley Periodicals, Inc. *J Polym Sci Part B: Polym Phys* 49: 1263–1268, 2011

KEYWORDS: block copolymers; carbon nanotubes; fullerenes; interfaces; photophysics

INTRODUCTION Conjugated polymers are currently used as a major component in organic photovoltaics (OPV) that are expected to provide low-cost, large-area, lightweight, and flexible alternative to silicon-based solar cells.^{1–3} A crucial issue in polymer-based OPV is control of the mesoscale morphology of the active layer. In bulk heterojunction (BHJ) configuration where donor-type-conjugated polymers (hole conducting) and acceptor-type fullerenes (electron conducting)² are mixed together, efficient charge collection requires that the donor and acceptor materials form an interpenetrating and continuous network, “phase separated” on the scale of the exciton diffusion length ~ 10 nm.⁴ It has been reported that BHJ solar cells comprising high-mobility donor polymers and a fullerene derivative, phenyl-C₆₁-butyric acid methyl ester (PCBM), as an electron acceptor, yield a power conversion efficiency of $\sim 8\%$.⁵

As the performance in BHJ OPV depends critically on the morphology of the active layer,^{6–8} and particularly on the intramolecular and intermolecular interactions between the polymer chains and the nanostructures, large efforts are being invested in the development of processing approaches that will enable the engineering of the mesoscale morphology.

Recently, it was suggested^{9,10} that the addition of carbon nanotubes (CNT) to the traditional mixture of fullerenes and conjugated polymers should improve the PV performance of the three-component system. This class of devices aims to take advantage of the electron-accepting feature of the fullerenes, and the high-electron transport capability of single walled carbon nanotubes (SWNT).¹¹ SWNT offer superior electron transport properties where reduced carrier scattering for hot carrier transport result in a near-ballistic

Additional Supporting Information may be found in the online version of this article.
Céline Bounioux and Racheli Itzhak contributed equally to this work.

© 2011 Wiley Periodicals, Inc.

transport along the tube.^{12,13} In addition, the high aspect ratio (length-to-diameter) $>10^3$ of SWNT yields percolation thresholds below 0.1 weight percent (wt %) ¹⁴ offering a high-mobility pathway for electron transport at minute bulk concentrations. Among the conjugated polymers, poly(3-hexylthiophene) (P3HT) is one of the promising materials due to the high charge carrier mobility (e.g., $0.1 \text{ cm}^2 \text{ V}^{-1} \text{ s}^{-1}$),¹⁵ and suitable light absorption in the visible range of the solar spectrum. In this system as well, the morphology of the active layer determines the optoelectronic properties of the devices.¹⁶

While of great potential, the morphological control of the combined SWNT-PCBM-P3HT system is a formidable task, as it is affected by the mutual interactions among the components, surface interactions, and the geometry of the components.^{17,18}

Here, we demonstrate that electrospinning may be used for preparation of composite microfibers of the three-component system leading to a higher degree of ordering in the processed polymer and alignment of the SWNT along the drawing direction of the fibers.

The electrospinning technique is based on electrostatic forces drawing a jet of a polymer solution, which experiences high extension due to electrostatically driven bending instability forming microfibers to nanofibers.^{19,20} The strong shear force induces stretching and alignment of the polymer chains, as well as coalignment of elongated additives such as CNT.²¹ Followed by fast quenching due to solvent evaporation, one is able to fabricate solid nanofibers of densely packed and oriented polymer chains. The combined system described above presents a special challenge for electrospinning: P3HT exhibits very low viscoelasticity in solutions²² and SWNT are hard to disperse in organic solvents that are good solvents for conjugated polymers.²³

In this article, we demonstrate that the difficulties described above may be overcome by utilizing a tailor-made block-copolymer,²³ comprising polyethylene oxide blocks and a central hexa-*p*-phenylene block $(\text{PEO})_n(\text{Ph})_6(\text{PEO})_n$ (where $n = 8, 24,$ and 44) for the dispersion of the nanostructures (fullerene derivatives and individual CNT) in a liquid phase, and the mediation of the interfacial interactions of the combined system. The preparation of microfibers is followed by structural and functional characterization where spectroscopic characterization indicates a higher degree of conjugation among the P3HT chains when compared with thin films, and efficient quenching of the photoluminescence.

EXPERIMENTAL

Dispersions of Single Walled Carbon Nanotubes

Dispersions of SWNT [Carbolex Inc. SWNT (AP) <http://carbolex.com>] were prepared in chloroform (anhydrous, Frutarom, Israel) solutions of the triblock copolymer: The block copolymer $(\text{PEO})_n(\text{Ph})_6(\text{PEO})_n$ (where $n = 8, 24,$ and 44) was dissolved to form solutions of 2 wt %. The solutions were mixed for 2–3 days using a magnetic stirrer or a roller.

A powder of SWNT was sonicated mildly (50 W, 43 KHz) for 1 h in the polymer solution. Following the sonication, the dispersions were centrifuged (at $\sim 3 \times 10^4 \text{ g}$ for 20 min) and the supernatant (the dispersion) was decanted from above the precipitate. The resulting dispersions were macroscopically homogeneous, with ink-like appearance. Their microscopic structure was characterized using transmission-electron microscopy (TEM).

PCBM (99%, Solenne BV, the Netherlands) solutions were prepared following a similar procedure.

Solutions and Dispersions for Electrospinning

The solutions of P3HT were prepared (under an inert nitrogen atmosphere) by addition of 30 mg P3HT (M_w 55–60,000, Catalog no. 4002-E, Rieke Special Polymers) to a mixture of anhydrous chloroform and anhydrous trichloroethylene (Frutarom, Israel), at solvent weight ratio of 94:6, and the solutions were stirred overnight. The solvent mixture was used to mediate the volatility of the solution. A minute concentration of a high-molecular weight poly(ethylene oxide) (PEO; $M_n = 4,000,000$, Aldrich) was used to enhance the viscoelasticity of the solutions and improve spinnability: PEO was dissolved in chloroform to a final concentration of 0.2 wt %, and a proper volume was added to the P3HT solutions to a final concentration of 0.02–0.04 wt %.

P3HT-PCBM and P3HT-PCBM-SWNT fibers and spin-coated films were prepared by mixing the pre-prepared solutions and dispersions: the dispersions (prepared as described above) were mixed with the chloroform–trichloroethylene solution of P3HT to the final weight ratio between the components, ranging from PCBM wt % of 0 to 50 (PCBM:P3HT).

Electrospinning

Electrospinning was carried out at room temperature in air at relative humidity of 56%, flow rate 1.5 mL h^{-1} . In a typical procedure for electrospinning, the solution was added to a plastic syringe connected to a stainless steel needle. The metallic needle was connected to a high voltage power supply (Gamma High Voltage, XRM30P) using a spinning voltage of 6–7 kV, and a grounded substrate was placed 12 cm below the tip of the needle to collect the fibers.²¹

Morphological Characterization

The morphology of the fibers was characterized using optical microscopy (Olympus BX51 a magnification of $\times 1000$, scale bar $500 \mu\text{m}$), high-resolution transmission electron microscopy (HRTEM, FEI Tecnai 12 G² TWIN TEM.), scanning electron microscopy (SEM, JEOL JSM-7400F), and scanning probe microscopy (SPM) in torsional resonance (TR), a noncontact technique (Digital Instruments Veeco, Dimension 3100 SPM). In this mode, lateral forces that act on the tip cause a change in the torsional resonant frequency, amplitude, and/or phase of the cantilever. AFM measurements at TR enable low-force scanning while maintaining the tip in the near-field and thus enabling the scanning of a soft sample such as P3HT-based fibers.

The specimens for TEM analysis were prepared by direct deposition of the electrospun nanofibers onto a copper grid coated

by a holey carbon film. In some of the samples, the composite fibers were etched using reactive ion etching with oxygen as the reactive gas. The exposure time ranged from 30 to 180 s.

Absorption and photoluminescence measurements (transmittance mode) were carried out using Varian Cary 100 spectrophotometer and Varian CARY ECLIPSE. Lambda 1050 UV/Vis/NIR narrow band spectrophotometer (PerkinElmer) equipped with 150-mm integrating sphere were used for measurements of P3HT fibers in the diffuse reflectance mode. For these measurements, the fibers were collected on gold-coated silicon wafer.

RESULTS AND DISCUSSION

Electrospinning was recently used for preparation of polymer-CNT composite nanofibers. It is known that the sink flow and the high extension of the electrospun jet align the nanotubes during the process when the SWNT are well dispersed in the polymer solution used for spinning.^{24,25} Thus, special emphasis was devoted to the preparation of high-quality dispersions.

Preparation of Dispersions

Dispersions of SWNT were prepared using a hexa-*p*-phenylene polyethylene oxide triblock copolymer, $(\text{PEO})_n(\text{Ph})_6(\text{PEO})_n$ ($\text{PEO})_n$ (where $n = 8, 24, \text{ and } 44$) in chloroform, following the procedure described above. As shown in a previous study,²³ the tailor-made block copolymer enables the preparation of stable, ink-like dispersions of individual SWNT in organic solvents [Fig. 1(a,b)] that are stable for long periods of time.

TEM of dried samples [Fig. 1(b)] and cryo-TEM imaging of the dispersions indicate that the dispersion mostly comprises individual SWNT. The need to preserve the electronic structure of the pristine SWNT excludes the use of covalently functionalized SWNT as functionalization transforms sp^2 -bonded carbons into sp^3 , and results in localization of the π electrons.²⁶ Steric repulsion among physically adsorbed polymers as described here does not impair the electronic structure of the pristine tubes.²⁷

Fibers of P3HT

To test the effect of electrospinning on the packing efficiency and crystallinity of the polymer, P3HT fibers were spun from a chloroform solution of P3HT. As reported before,²² the addition of a high-molecular weight flexible polymer to the P3HT solutions is necessary for the onset of a stable jet and the formation of fibers. In this study, we used a low concentration (0.02–0.04 wt %) of a high molecular weight PEO (M_w 4,000,000 g mol^{-1} , Aldrich; C/C^* is between 1.5 and 2.4). Continuous, long fibers of micrometric diameter were collected [Fig. 2(a,b)].

The absorption of pristine P3HT fibers collected on gold-coated glass was investigated and compared to that of spin-cast P3HT films (final thickness of 300 nm), prepared from the very same solution used for the spinning. As observed in Figure 2(c) λ_{max} (films) = 515 nm while λ_{max} (fibers) = 580 nm. The observed red-shift in the absorption spectra of the P3HT fibers at round 600 nm, when compared with the spin-coated films, is indicative for a longer

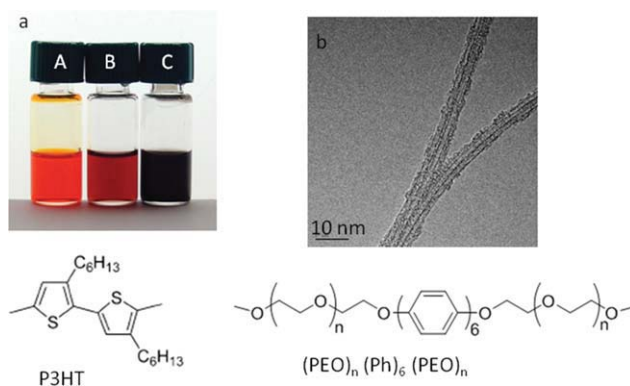


FIGURE 1 (a) Solutions in chloroform of (A) P3HT M_w 55–60,000 (3 wt %), (B) PCBM (5 wt %), and (C) a dispersion of SWNT (1 wt %) in an anhydrous chloroform solution of $(\text{PEO})_8(\text{Ph})_6(\text{PEO})_8$ (2 wt %). Similar dispersions were obtained using $(\text{PEO})_{44}(\text{Ph})_6(\text{PEO})_{44}$. (b) A TEM image of SWNT dispersion (1 wt %) in a chloroform solution of $(\text{PEO})_8(\text{Ph})_6(\text{PEO})_8$ (2 wt %).

conjugation length and a reduction of the steric hindrance due to alkyl side chains. Both result from the strong stretching and elongation of the polymer chains during the spinning process²⁸ and lead to a closer packing of the chains in the fibers when compared with the films.²⁹ Furthermore, SPM images [Fig. 2(d)] show features that may be interpreted³⁰ as mesoscale ordered isolated microwires and whiskers. Crystallization along the draw axis is expected to occur due to the stretching of the confined polymer chains in the fibers.³¹

Fibers of PCBM–P3HT

When attempting to electrospin mixtures of P3HT and PCBM, the mixtures strongly aggregated, and rather than forming uniform cylindrical-like fibers, beading was observed. As presented in Figure 3(a), the beads were of macroscopic size and appeared at a high frequency along the fibers.

It is known¹⁹ that the solution properties such as viscosity, viscoelasticity, surface tension, and electrical conductivity, as well as the flow rate, affect the morphology and diameter of the fibers, as well as the stability of the electrospinning process. We hypothesized that the beads present in the fibers are due to nanoparticles agglomerations in the PCBM–P3HT mixture under the spinning conditions. To mediate the interfacial interactions, the hexa-*p*-phenylene polyethylene oxide triblock copolymer, $(\text{PEO})_n(\text{Ph})_6(\text{PEO})_n$ used for dispersion of SWNT was added to the PCBM–P3HT mixture, at a similar concentration used for SWNT dispersions (2 wt %). Indeed, we found that bead-free micron long fibers could be formed, as presented in Figure 3(b).

Fibers of SWNT–PCBM–P3HT

Fibers of SWNT–PCBM–P3HT were prepared by electrospinning dispersions of the three components in chloroform solutions of the block copolymer $(\text{PEO})_n(\text{Ph})_6(\text{PEO})_n$. We found that predispersion of the SWNT in solutions of the block copolymer followed by addition of a solution of the predissolved PCBM and a solution of the predissolved P3HT enabled the formation of micron long fibers with a diameter ranging between 0.5 and

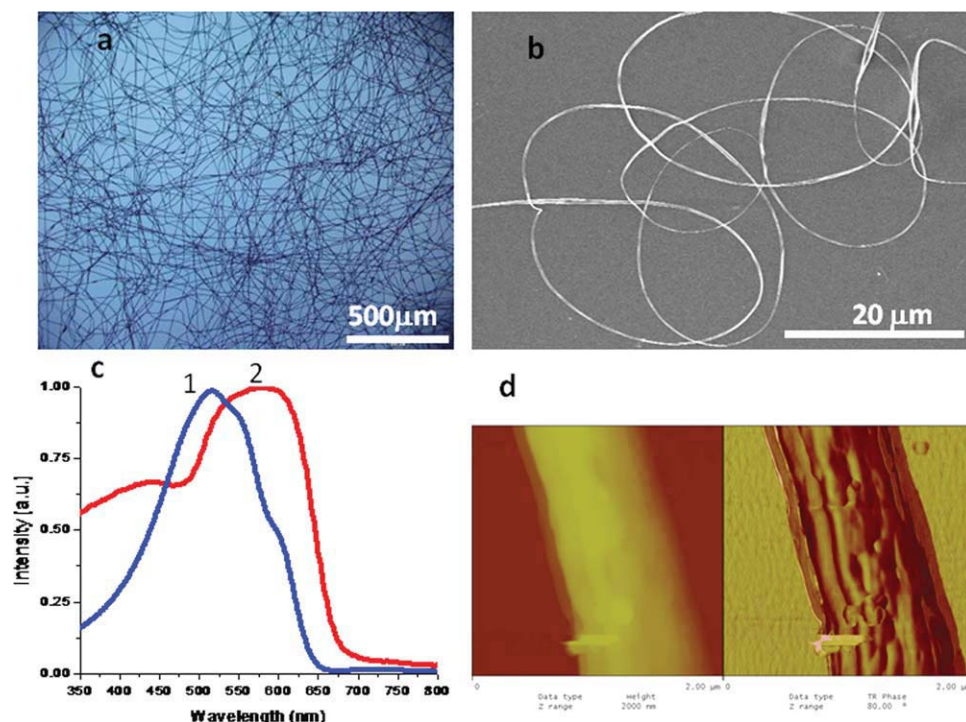


FIGURE 2 Images of P3HT-PCBM (5 wt %)-SWNT (1 wt %) fibers prepared via electrospinning following the procedure described in the text. (a) Optical image of fibers collected on glass, scale bar 50 μm . (b) SEM image of a fiber. (c) Absorption of P3HT films (blue) and fibers (red) prepared from a solution of 3 wt % P3HT and 0.02 wt % PEO in anhydrous chloroform. Films were spin coated onto glass substrates to a final thickness of about 300 nm. (d) Scanning probe microscopy (SPM) image taken in torsional resonance, a noncontact technique, of fibers collected onto a silicon wafer. Topography (left, Z range 2000 nm) and phase (right, Z range 30°). The full scale is 2 μm .

2 μm , depending on the relative concentrations of the different components, as presented in Figure 4(a).

The TEM images presented in Figure 4(b,c) substantiate the presence of SWNT in the three-component fibers. As the contrast between the conjugated polymer and the SWNT is not high enough, we used oxygen plasma to sputter away most of the fiber. Figure 4(b,c) demonstrate the presence of small bundles of SWNT. Indeed, previous studies²⁴ indicate that

well-dispersed CNT may be incorporated as individual elements mostly aligned along the nanofiber axis in aqueous solutions of spinnable polymers.

Photoluminescence in P3HT, P3HT-PCBM, and P3HT-PCBM-SWNT Fibers

Photoluminescence (PL) spectra of different fibers were measured to probe the electronic interactions among the components. The PL spectra of pristine P3HT films and fibers

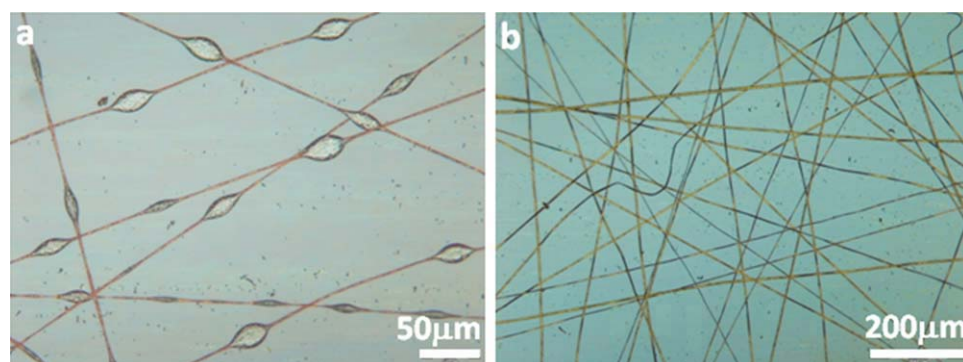


FIGURE 3 (a) An optical image of P3HT-PCBM fibers prepared from a solution, which does not contain the dispersing block copolymer (b) An optical image of fibers prepared from dispersions of P3HT + PCBM (5 wt %) + block-copolymer (2 wt %). The concentrations of the additives are normalized to 30 mg mL^{-1} P3HT.

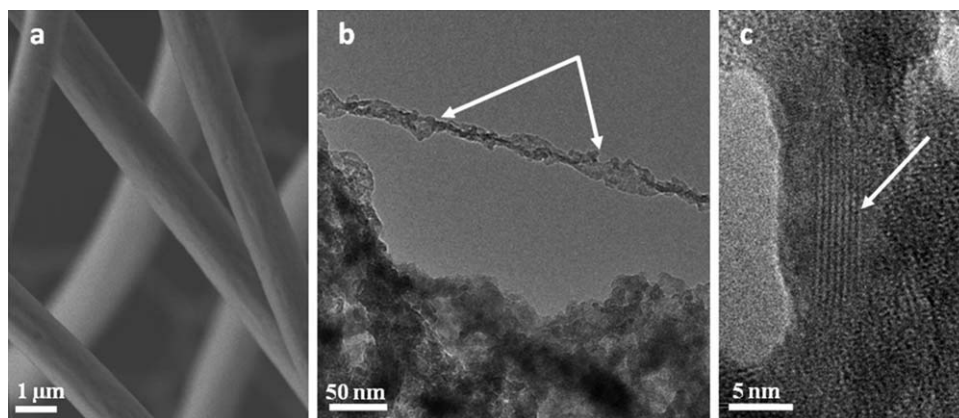


FIGURE 4 EM images of P3HT–PCBM (15 wt %) – SWNT (1 wt %) + block-copolymer (2 wt %) fibers. (a) SEM image showing the as-spun fiber. (b) HRTEM image following oxygen sputtering of the collected sample. The arrow points to a SWNT embedded in the fiber. (c) A HRTEM image showing a SWNT bundle (white arrow) embedded within a P3HT fiber. The concentrations of the additives are normalized to 30 mg mL^{-1} P3HT.

are shown by curves 1 and 2, respectively, in Figure 5(a). The introduction of 33 wt % of PCBM into the P3HT films and fibers [curves 3 and 4 in Fig. 5(a)] are demonstrated to result in a significant quenching of the PL in both samples. The PL spectra for fibers of PCBM–P3HT–block-copolymer and SWNT–PCBM–P3HT–block-copolymer [Fig. 5(b)] show a similar trend. Figure 5(c) shows that the reduction in PL intensity increases with increasing PCBM concentration in the fibers. In a “conjugated polymer–fullerene” system, these findings are known to indicate an efficient electron transfer at the polymer–PCBM interface.³² These results suggest that the presence of the block-copolymer does not affect the efficiency of the electron transfer at the P3HT–PCBM interface in PCBM–P3HT and SWNT–PCBM–P3HT fibers.

To summarize, we demonstrated the preparation of SWNT–PCBM–P3HT fibers via electrospinning and characterized their structure and spectroscopic properties. The formation of these functional fibers was enabled by the utilization of a triblock copolymer (poly(ethylene oxide)-(hexa-*p*-phenylene)-poly(ethyleneoxide)) for mediating the interactions among the PCBM and SWNT in the solution used for spinning. In the presence of the block copolymer, the spinning process results in the formation of long uniform fibers with a typical diameter below a micron. The findings presented here indicate that flow-induced stretching of the P3HT chains together with the incorporated SWNT along the fiber that result in a red-shift in the absorbance spectra of the fibers, may indicate an increased ordering of the polymer in the

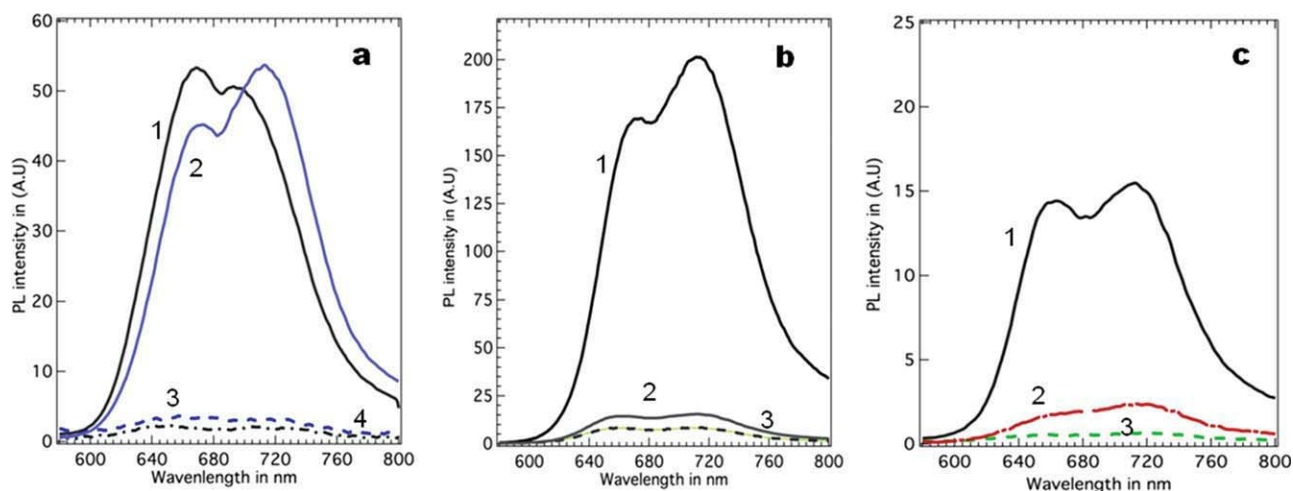


FIGURE 5 PL spectra (excited at 452 nm) of different sets of P3HT-based fibers and films. (a) Curve 1, P3HT film; curve 2, P3HT fiber; curve 3, film of (P3HT + 33% PCBM); curve 4, fiber of (P3HT + 33% PCBM). (b) Curve 1, fiber of [P3HT + block-copolymer (2 wt %)], curve 2, fiber of [P3HT + PCBM (5 wt %) + block-copolymer (2 wt %)]; curve 3, fiber of [P3HT + PCBM (5 wt %) + SWNT (1 wt %) + block-copolymer (2 wt %)]. (c) Fibers of [P3HT + Block-copolymer (2 wt %) + different concentrations of PCBM]: curve 1, 5 wt % of PCBM; curve 2, 25 wt % of PCBM, curve 3, 40 wt % of PCBM. Concentrations of the additives are normalized to 30 mg mL^{-1} P3HT.

fibers when compared with spin-cast films. The strong PL quenching in the SWNT-PCBM-P3HT fibers points out to the efficient charge transfer in these nanocomposites.

These findings may open a novel research avenue for the utilization of fibers of functional nanocomposites, in particular, in BHJ OPV cells. For instance, it makes possible to unify in a single solar panel, the three recently suggested strategies in OPV development: BHJ solar cells based on individual fibers³²; photovoltaic textile-based solar panels,^{33,34} and OPV cells with conductive mesh grids (ITO-free devices).^{35,36} Figure S1 (in Supporting Information) illustrates a possible example of such device architecture.

The development of such or similar fiber-based devices will raise new research challenges, the most important of which deal with optimization of the fiber diameter in connection with their electrical and mechanical properties. The thickness of the photoactive layer in conventional BHJ cells is usually of ~ 100 nm. This thickness reflects a trade-off between the light absorption and poor electronic transport. Although the introduction of CNT and the corresponding modification of electronic transport in the cell photoactive layer may shift the result of this trade-off toward higher thickness, optimization of the technological conditions to produce fibers with smaller diameters should be an important topic in further research. On the other hand, the principle of BHJ allows to increase the thickness of blend films for maximizing the sunlight absorption if an optimum charge percolation path can be still maintained.^{37,38} In particular, Lee et al.³⁹ demonstrated recently a half-a-micron thick efficient P3HT:PCBM BHJ cell.

ACKNOWLEDGMENT

The work was funded by the Focal Initiatives in Science and Technology (FIRST) foundation of the Israel Science Foundation grant no. 1004/07 R.Y.R holds the Stanley D. and Nikki Waxberg professorial chair in Advanced Materials.

REFERENCES AND NOTES

- Brabec, C. J.; Sariciftci, N. S.; Hummelen, J. C. *Adv. Funct. Mater.* **2001**, *11*, 15–26.
- Yu, G.; Gao, J.; Hummelen, J. C.; Wudl, F.; Heeger, A. J. *Science* **1995**, *270*, 1789–1791.
- Krebs, F. C. *Sol. Energy Mater. Sol. Cells* **2009**, *93*, 394–412.
- Halls, J. J. M.; Pichler, K.; Friend, R. H.; Moratti, S. C.; Holmes, A. B. *Appl. Phys. Lett.* **1996**, *68*, 3120–3122.
- Brabec, C. J.; Gowrisanker, S.; Halls, J. J. M.; Laird, D.; Jia, S.; S. P. Williams, S. P. *Adv. Mater.* **2010**, *22*, 3839–3856.
- Oosterhout, S. D.; Wienk, M. M.; Bavel, S. S. V.; Thiedmann, R.; Koster, L. J. A.; Gilot, J.; Loos, J.; Schmidt, V.; Janssen, R. A. *J. Nat. Mater.* **2009**, *8*, 818–824.
- Zhao, J.; Swinnen, A.; Assche, G. V.; Manca, J.; Vanderzande, D.; Mele, B. V. *J. Phys. Chem. B* **2009**, *113*, 1587–1591.
- Kim, J. S.; Park, Y.; Lee, D. Y.; Lee, J. H.; Park, J. H.; Kim, J. K.; Cho, K. *Adv. Funct. Mater.* **2010**, *20*, 540–545.
- Li, C.; Chen, Y.; Wang, Y.; Iqbal, Z.; Chhowalla, M.; Mitra, S. *J. Mater. Chem.* **2007**, *17*, 2406–2411.
- Liu, L.; Stanchina, W. E.; Li, G. *Appl. Phys. Lett.* **2009**, *94*, 233309–233311.
- Dresselhaus, M. S.; Dresselhaus, G.; Avouris, Ph. *Topic. Appl. Phys.* **2001**, *80*, 1–9.
- White, C. T.; Todorov, T. N. *Nature* **1998**, *393*, 240–242.
- Martel, R.; Avouris, P. *Nano Lett.* **2004**, *4*, 1063–1066.
- Grujicic, M.; Cao, G.; Roy, W. N. *Mater. Sci.* **2004**, *39*, 4441–4449.
- Bao, Z.; Dodabalapur, A.; Lovinger, A. *J. Appl. Phys. Lett.* **1996**, *69*, 4108–4110.
- Chen, L.-M.; Hong, Z.; Li, G.; Yang, Y. *Adv. Mater.* **2009**, *21*, 1434–1449.
- Peng, G.; Qiu, F.; Ginzburg, V. V.; Jasnow, D.; Balazs, A. C. *Science* **2000**, *288*, 1802–1804.
- Buxton, G. A.; Balazs, A. C. *Mol. Simul.* **2004**, *30*, 249–257.
- Huang, Z.-M.; Zhang, Y.-Z.; Kotaki, M.; Ramakrishna, S. *Compos. Sci. Technol.* **2003**, *63*, 2223–2253.
- Theron, S. A.; Zussman, E.; Yarin, A. L. *Polymer* **2004**, *45*, 2017–2030.
- Salalha, W.; Dror, Y.; Khalfin, R. L.; Cohen, Y.; Yarin, A. L.; Zussman, E. *Langmuir* **2004**, *20*, 9852–9855.
- Laforgue, A.; Robitaille, L. *Synthetic Met.* **2008**, *158*, 577–584.
- Itzhak, R.; Raichman, D.; Shahar, Z.; Frey, G. L.; Frey, J.; Yerushalmi-Rozen, R. *J. Phys. Chem. C* **2010**, *114*, 3748–3753.
- Dror, Y.; Khalfin, R. L.; Cohen, Y.; Yarin, A. L.; Zussman, E. *Langmuir* **2003**, *19*, 7012–7020.
- Salalha, Y.; Dror, Y.; Khalfin, R. L.; Cohen, Y.; Yarin, A. L.; Zussman, E. *Langmuir* **2004**, *20*, 9852–9855.
- López-Bezanilla, A.; Triozon, F.; Latil, S.; Blase, X.; Roche, S. *Nano Lett.* **2009**, *9*, 940–944.
- Szleifer, I.; Yerushalmi-Rozen, R. *Polymer* **2005**, *46*, 7803–7818.
- Arinstein, A.; Burman, M.; Gendelman, O.; Zussman, E. *Nat. Nanotechnol.* **2007**, *2*, 59–62.
- Chuangchote, S.; Fujita, M.; Sagawa, T.; Sakaguchi, H.; Yoshikawa, S. *Appl. Mater. Interfaces* **2010**, *2*, 2995–2997.
- Grévin, B.; Rannou, P.; Payerne, R.; Pron, A.; Travers, J. P. *J. Chem. Phys.* **2003**, *118*, 7097–7102.
- Howard, I. A.; Mauer, R.; Meister, M.; Laquai, F. *J. Am. Chem. Soc.* **2010**, *132*, 14866–14876.
- Lee, M. R.; Eckert, R. D.; Forberich, K.; Dennler, G.; Brabec, C. J.; Gaudiana, R. A. *Science* **2009**, *324*, 232–235.
- Bedelogleu, A.; Koeppe, R.; Demir, A.; Bozkurt, Y.; Sariciftci, N. S. *Fibers Polym.* **2010**, *11*, 378.
- Bedelogleu, A.; Demir, A.; Bozkurt, Y.; Sariciftci, N. S. *Text. Res. J.* **2010**, *80*, 1065–1074.
- Kylberg, W.; de Castro, F. A.; Chabreck, P.; Sonderegger, U.; Chu, B. T.-T.; Nüesch, F.; Hany, R. *Adv. Mat.* **2011**, *23*, 1015–1019.
- Galagan, Y.; Rubingh, J.-E. J. M.; Andriessen, R.; Fan, C.-C.; Blom, P. W. M.; Veenstra, S. C.; Kroon, J. M. *Sol. Energy Mater. Sol. Cells* **2011**, *95*, 1339–1343.
- Dennler, G.; Scharber, M. C.; Brabec, C. J. *Adv. Mater.* **2009**, *21*, 1323–1338.
- Servaites, J. D.; Ratner, M. A.; Marks, T. J. *Appl. Phys. Lett.* **2009**, *95*, 1–3.
- Lee, S.; Nam, S.; Kim, H.; Kim, Y. *Appl. Phys. Lett.* **2010**, *97*, 1–3.